Journal of Thermal Analysis and Calorimetry, Vol. 91 (2008) 3, 957–962

SPECTRAL AND THERMAL STUDIES OF NEW Co(II) AND Ni(II) HEXAAZA AND OCTAAZA MACROCYCLIC COMPLEXES

M. Gaber[*], *A. F. Rehab and D. F. Badr-Eldeen*

Chemistry Department, Faculty of Science, Tanta University, Tanta, Egypt

The macrocyclic complexes of Co(II) and Ni(II) having chloride or thiocyanate ions in the axial position have been synthesized and characterized. These complexes are synthesised by the template condensation of *o*-phenylenediamine or 2,3-butanedionedihydrazone with the appropriate aldehydes in NH_4OH solution in the presence of the metal ions, Co(II) and Ni(II). The complexes were characterized by spectroscopic methods (IR, UV-Vis and ESR) and magnetic measurements as well as thermal analysis (TG and DTA). The results obtained are commensurate with the proposed formulae. Spectral studies indicate that these complexes have an octahedral structure. From conductivity measurements the complexes are non-electrolytes. The kinetic of the thermal decomposition of the complexes was studied and the thermodynamic parameters are reported.

Keywords: *Co(II), Ni(II), macrocyclic complexes, template condensation, thermal analysis*

Introduction

The development of the field of bioinorganic chemistry plays an important generating interest in macrocyclic compounds and their metal complexes. Transition metal macrocyclic complexes have received much attention as an active part of metalloenzymes [1] as biomimic model compounds [2]. In recent years, a great deal of interest has been directed towards the metal-controlled template synthesis of macrocyclic species [3–5]. Very few systems have been reported for the macrocyclic metal complexes showing the correlation btween the thermal stability and the structures of the macrocyclic metal complexes [6, 7].

In this paper, we report the synthesis and characterization of new hexaaza- and octaaza-macrocyclic complexes prepared by template condensation reactions of *o*-phenylene-diamine or 2,3-butanedione dihydrazone with formaldehyde and glutaraldehyde respectively, in the presence of Co(II) and Ni(II) ions. The complexes were characterized based on elemental analyses, IR, UV-Vis, ESR, magnetic moments and molar conductance measurements. The thermal behaviour of these complexes was studied by TG and DTA. The kinetics of the thermal decomposition was studied and the kinetic thermal parameters were calculated.

Experimental

All chemical used were of chemically pure grade. 2,3-butanedione dihydrazone was prepared according to the published procedure [8].

Macrocyclic cobalt(II) complex

An alcoholic solution of *o*-phenylenediamine (0.02 mol) was degassed by passing purified nitrogen in a three-necked flask and a degassed ethanolic solution of Co(II) chloride (0.01 mol) was added slowly with stirring followed by the addition of (0.04 mol) of formaldehyde to the mixture. The reaction mixture was warmed and stirred, then ammonia solution (0.02 mol) was added dropwise with stirring. The mixture was stirred for 8 h, cooled and the product was filtered off, washed with petroleum ether then dried in vacuum over P_2O_5. Yield is found to be about 80%.

Attempts to prepare the thiocyanate and perchlorate derivatives by the addition of potassium thiocyanate solution and perchloric acid to the Co(II) complex were unsuccessful.

Macrocyclic nickel(II) complexes

Hexaaza macrocyclic complex

An ethanolic solution of the *o*-phenylene diamine (0.02 mol in 20 mL) was degassed with nitrogen in a three-necked flask. A degassed solution of Ni(II) chloride (0.01 mol) in 10 mL ethanol was added dropwise with stirring. The mixture was stirred, then (0.02 mol) of formaldehyde was slowly added followed by the addition of (0.02 mol) ammonia solution. The mixture was warmed and stirred for 12 h. The brown precipitate obtained was filtered off, washed with petroleum ether and dried in vacuum over P_2O_5. Yield was found to be 80%.

---

[*] Author for correspondence: abuelazm@yahoo.com

1388–6150/$20.00

Akadémiai Kiadó, Budapest, Hungary
Springer, Dordrecht, The Netherlands

Attempts to prepare Cu(II) macrocyclic complex was unsuccessful. Also, attempts to prepare the nickel thiocyanate and perchlorate derivatives were unsuccessful.

Octaaza macrocyclic complex

Firstly, an alcoholic solution of 2,3-butanedione dihydrazone (0.02 mol in 20 mL) was warmed and a degassed ethanolic solution of Ni(II)acetate (0.02 mol in 10 mL) was then added dropwise with stirring followed by the addition of glutaraldehyde (0.02 mol).

The mixture was degassed by passing purified nitrogen in a three-necked flask and stirred for about 12 h; then an aqueous solution of KNCS (0.02 mol) was slowly added and the mixture was stirred for 6 h. The formed precipitate was filtered off, washed with petroleum ether and dried in vacuum over P_2O_5. Yield was 55%.

The metal content in the macrocyclic complexes was determined by digesting an accurately weighed amount of the solid complex in (1:1) $HClO_4$ until all the fumes of $HClO_4$ had ceased to evolve, then transferred into a measuring flask and titrating a known volume with EDTA. The results were further confirmed from the TG data.

Instrumental methods

Microanalysis C, H and N for the complexes were carried out using Heraeus CHN elemental analyzer. The molar conductance of the solid complexes in DMF (10^{-3} M) were also measured using conductance bridge of the type 523 conductance meter. The IR spectra were recorded on a Perkin Elmer 1430 spectrometer in a KBr matrix within the 4000–200 cm^{-1} region.
The thermal analysis (TG and DTA) were recorded under N_2 flow (20 mL min^{-1}) on Shimadzu TG-50 equipment at heating rate 10°C min^{-1}. The electronic absorption spectra were recorded by the aid of Shimadzu 240 spectrophotometer. Magnetic susceptibilities were measured by the Gouy method at room temperature using a magnetic susceptibility balance (Johnson Matthey Alfa Product, Mod. MKI). Diamagnetic corrections were calculated from Pascal's constants. The ESR spectra were recorded on a JEOL JEX-FE 2XG spectrometer.

Kinetic data

All the well-defined stages were selected for the study of the kinetics of decomposition of the complexes. The kinetic parameters like the activation energy (E) and the pre-exponential factor (A) were calculated using Coats–Redfern equation [9];

$$\ln[g(\alpha)/T^2]=\ln(AR/QE)[1-(2RT_c/E)]-E/RT$$

where T is the temperature, Q is the heating rate (10°C min^{-1}), R is the gas constant and T_c is mean temperature of the original data.

A plot of $\ln[g(\alpha)/T^2]$ *vs.* $1/T$ gave straight lines whose slopes and intercepts were used to evaluate E and A, respectively. The goodness of fit was checked by calculating the correlation coefficient. The assignment of the mechanism of the thermal decomposition is based on the assumption that the form of $g(\alpha)$ depends on the reaction mechanism. In the present study, the nine forms of $g(\alpha)$ suggested by Satava [10] were used to enunciate the mechanism of thermal decomposition in each step. The value of $g(\alpha)$ with highest correlation coefficient is taken as the mechanism of thermal decomposition. The entropy of activation (ΔS), enthalpy of activation (ΔH) and the free energy change of activation (ΔG) were calculated using the following equations:

$$\Delta S=2.303R\log(Ah/kT)$$

$$\Delta H=E-RT$$

$$\Delta G=H-T\Delta S$$

where k and h are the Boltzman and Plank constants, respectively.

Results and discussion

All the prepared complexes were subjected to elemental analysis. The complexes were found to be of low molar conductance values (14.4, 12 and 13.6 ohm^{-1} cm^2 mol^{-1} for complexes **1**, **2** and **3**, respectively) indicating the coordination nature of Cl^- or NCS^- ions and confirming the nonelectrolyte nature of these complexes [11]. The analytical and spectral data for all complexes are listed in Tables 1 and 2, respectively.

Table 1 Elemental analysis of new synthetic macrocyclic complexes

No.	Suggested formula	Colour	Microanalysis results/Calc. (found)			
			C/%	H/%	N/%	M/%
1	$[CoLCl_2]\cdot 2(H_2O)$	dark brown	41.29 (41.57)	5.59 (5.78)	18.07 (18.46)	12.69 (12.35)
2	$[NiLCl_2]\cdot 2(H_2O)$	dark brown	41.41 (41.09)	5.61 (5.43)	18.12 (17.96)	12.66 (12.23)
3	$[NiL(SCN)_2]\cdot(H_2O)$	olive green	43.11 (43.00)	6.83 (6.25)	25.15 (25.22)	10.54 (10.41)

Table 2 IR, electronic absorption, ESR spectral data and magnetic moment values of new synthetic macrocyclic complexes

No	IR spectra/cm^{-1}						λ_{max}/ nm	ESR spectra			μ_{eff}/ BM
	OH	NH	CH_2[a]	C–N[b]	C–N	M–N		$g_{\parallel}$	$g_{\perp}$	g_{eff}	
1	3548	3416	1461	1240	1104	425	410, 550	2.608	1.992	2.197	4.30
2	3544	3247	1468	1263	1043	448	430, 580	–	–	–	3.17
3	3546	3326	–	–	1097	–	440, 560	–	–	–	3.01

[a]in ring formation; [b]aromatic

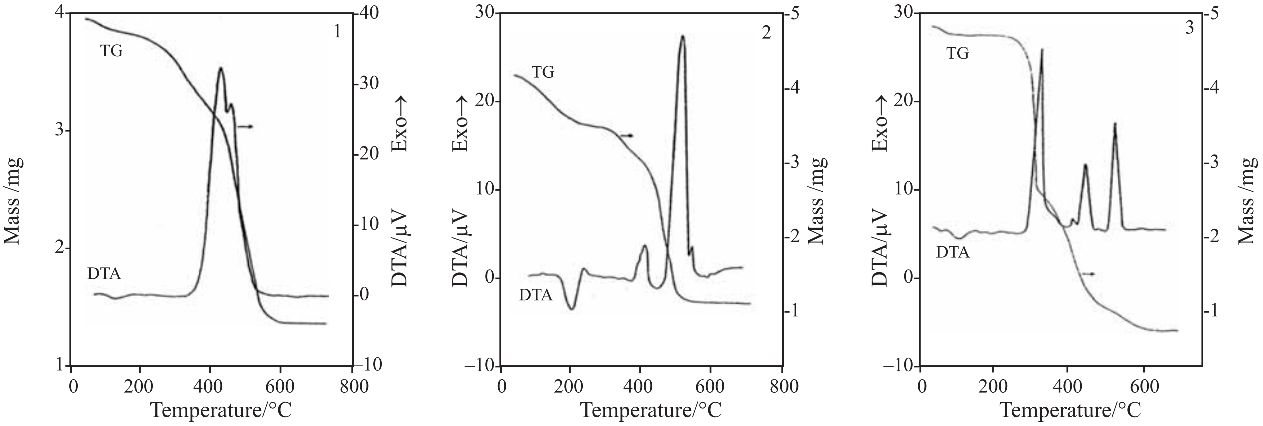

Fig. 1 TG and DTA curves for complexes **1**–**3**

Co(II) complex

The thermal analysis of the Co(II) complex is shown in Fig. 1. The observed mass loss within the temperature range 100–150°C associated with an endothermic peak at 130°C could be correlated with the removal of the non-coordinated water molecules; hence the number of water molecules was calculated and found to be two. The chloride ions were lost within the temperature range 220–400°C. Above 400°C the mass loss associated with an exothermic peak at 390°C corresponded to the decomposition of the complex with the formation of Co_2O_3 from which the metal content was calculated and found to be in confirmity with that obtained from elemental analysis. Based on the thermal analysis, the decomposition of Co(II) complex can be represented as follows:

$$[CoLCl_2]\cdot 2H_2O \xrightarrow{100-150°C} [CoLCl_2] \xrightarrow{220-400°C}$$
$$CoL \xrightarrow{>400°C,\ oxidation} Co_2O_3$$

The plot of $\ln[g(\alpha)/T^2]$ functions *vs.* $1/T$ was drawn for Co(II) complex **1** (Fig. 2) as an example; it was found that the first stage could be best described by R3 mechanism, where chemical decomposition controls. The second stage showed extremely close maximum values of correlation coefficients R for all mechanisms (>0.99), so that it was possible to decide which is controlling (Table 3). The third step showed two close maximum values for mechanisms D2 and D3. Since the latter corresponds to diffusion through spherical product shell, it was thought to be more probable than the former (which corresponds to cylindrical shapes). So, the probable mechanism is D3. The kinetic parameters are listed in Table 4. There is no definite trend observed in the values of E and ΔS for the different stages of decomposition. The *–ve* values of entropy of activation indicate that the activated complex has a more ordered structure than the reactants [12, 13].

For the anhydrous Co(II) complex, the value of E is higher for the third stage of decomposition compared to that of the second stage indicating that the third stage is more ordered than the second one. This may be expected due to the decreased steric strain when the ligand molecule is decomposed. The activa-

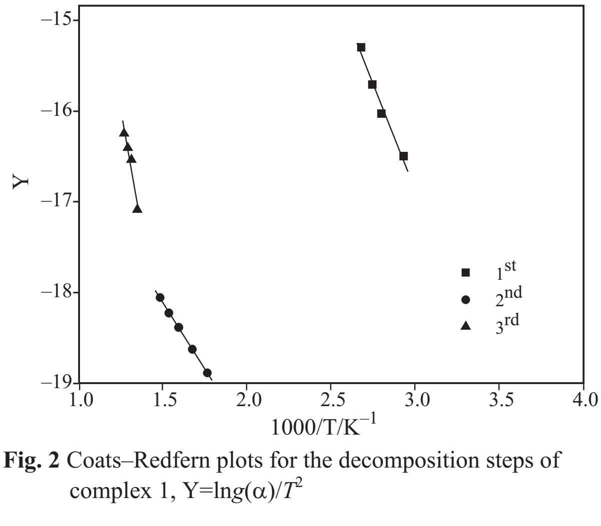

Fig. 2 Coats–Redfern plots for the decomposition steps of complex 1, $Y=\ln g(\alpha)/T^2$

Table 3 Correlation coefficients calculated for Co(II) and Ni(II) complexes using nine forms of $g(\alpha)$

Function	Forms of (α)	Complex **1**			Complex **2**			Complex **3**		
		I	II	III	I	II	III	I	II	III
D1	α^2	–0.984	–0.9993	–0.986	–0.727	–0.936	0.985	0.977	–0.982	–0.993
D2	$(1-\alpha)\ln(1-\alpha)+\alpha$	–	–0.9992	–0.987	–0.991	–0.978	0.815	0.974	–0.981	–0.996
D3	$[1-(1-\alpha)^{1/3}]^2$	–0.986	–0.9999	–0.988	–0.865	–0.984	0.989	0.977	0.984	0.996
R2	$1-(1-\alpha)^{1/2}$	–0.986	–0.998	–0.977	–0.969	–0.848	0.987	0.976	0.9785	–0.995
R3	$1-(1-\alpha)^{1/3}$	–0.989	–0.993	–0.982	–0.961	–0.681	0.989	0.976	–0.983	–0.998
F1	$-\ln(1-\alpha)$	–0.985	–0.997	–0.984	–0.947	0.299	≈–1.0	–0.98	–0.987	–0.995
A2	$-\ln(1-\alpha)^{1/2}$	–0.982	–0.993	–0.969	–0.998	0.991	0.987	0.967	–0.974	–0.947
A3	$-\ln(1-\alpha)^{1/3}$	–0.974	–0.999	–0.897	–0.996	–0.999	0.997	0.959	–0.965	0.777
A4	$-\ln(1-\alpha)^{1/4}$	–0.962	–0.9998	–0.888	–0.9998	–0.998	–0.47	0.947	–0.944	0.954

Table 4 Kinetic parameters obtained by the Coats–Redfern equation

No.	Stage	Fun.	E/kJ mol^{-1}	A/s^{-1}	$-\Delta S$/J K^{-1} mol^{-1}	ΔH/kJ mol^{-1}	ΔG/kJ mol^{-1}
1	I	R_3	38.98	3.6×10^5	146.3	32.7	143.3
	II	D_3	24.4	1.2×10^{10}	53.4	21.43	40.6
	III	D_3	84.9	4.8×10^4	161.4	78.9	179.4
2	I	A_4	5.3	3.2×10^9	65.3	2.07	27.6
	II	A_3	7.3	8.3×10^9	61.4	1.97	46.5
	III	F_1	40.1	5.6×10^5	142.6	33.9	146.5
3	I	F_1	44	8.1×10^4	152	41.3	93.3
	II	F_1	87.54	6×10^6	120	82.9	150.3
	III	R_3	15.2	8.8×10^8	80.4	9.62	63.54

(Fun.): F1 – random nucleation; D3 – three-dimensional diffusion, spherical symmetry Jander equation; R3 – phase boundary reaction contracting volume spherical symmetry; A3 and A4 – random nucleation Avrami equation II (n=3) and (n=4), respectively

tion energy of decomposition reaction is in the range 24.4–84.9 kJ mol^{-1} which indicates that the metal-ligand bond is very weak [14].

The IR spectrum of the Co(II) macrocyclic complex showed a shoulder at 3548 cm^{-1} and a band at 3416 cm^{-1} attributable to stretching vibration of non-coordinated water molecules and bonded NH group, respectively. The spectrum showed strong absorption bands at 1461 and 845 cm^{-1} which are caused by CH_2 deformation and rocking modes. The absorption band at 425 cm^{-1} can be assigned to the stretching vibration of Co–NH.

The Co(II) complex has a magnetic moment value equals to 4.13 BM which is consistent with the reported value for the octahedral Co(II) complex [15]. The electronic spectrum, in Nujol mull, exhibited two bands at 410 and 550 nm which may be assigned to $^4T_{1g}(F)\rightarrow{}^4T_{1g}(P)$ (υ_3) and $^4T_{1g}(F)\rightarrow{}^4T_{2g}(F)$ (υ_2) transitions, respectively indicating the octahedral environment. The ESR spectrum of the solid Co(II) complex at room temperature showed hyperfine splitting with g-values of $g_{\parallel}=2.608$ and $g_{\perp}=1.992$. The average g-value was found to be 2.197 i.e. above the free ion value (2.0023) which indicates that the metal-ligand bond is more covalent than ionic [16].

Ni(II) complexes

The analytical data of the Ni(II) complexes **2** and **3** along with other physical properties are listed in Table 1. The conductance values in DMF solution show the non-ionic nature of the complexes [11].

The curves of the Ni(II) complex **2** showed that the mass loss step takes place between 50–150°C corresponding to loss of two molecules of hydration water. This step is associated with an endothermic peak at 200°C. The second mass loss step occurring between 300–400°C with an exothermic peak at 400°C is due to the loss of Cl^- ions. The final mass loss stage between 400–510°C associated with a strong exothermic peak at 510°C is attributed to the decomposition of the complex along the chelate bond leading to the final product (NiO) from which Ni(II) content can be calculated.

$$[\mathrm{NiLCl_2}]{\cdot}2\mathrm{H_2O}\xrightarrow{50\text{–}150^\circ\mathrm{C}}[\mathrm{NiLCl_2}]\xrightarrow{300\text{–}400^\circ\mathrm{C}}\mathrm{NiL}\xrightarrow{400\text{–}510^\circ\mathrm{C}}\mathrm{NiO}$$

For the Ni(II)–complex **3** there is a loss of hydration water molecule below 100°C. This step is associated with a weak endothermic peak at ~100°C. The second mass loss is associated with a strong exothermic peak at 300°C corresponding to the loss of NCS^- ions. The third mass loss step takes place within the temperature range 350–700°C associated with exothermic peaks at 400–500°C. This temperature range corresponds to the decomposition of the complex with the formation of NiO as a final product.

$$[\mathrm{NiL(NCS)_2}]{\cdot}\mathrm{H_2O}\xrightarrow{25\text{–}100^\circ\mathrm{C}}[\mathrm{Ni(NCS)_2}]\xrightarrow{250\text{–}300^\circ\mathrm{C}}\mathrm{NiL}\xrightarrow{>300}\mathrm{NiO}$$

The results of the kinetic analysis for the thermal decomposition of the Ni(II)–complex **2** show that the linear correlation coefficients are better when the probable mechanism functions are used; A4 for the first, A3 for the second and F1 for the third stage of decomposition. The significance of A4, A3 and F1 is listed in Table 4. For Ni(II)–complex **3** the most probable mechanisms are F1, F1 and R3 for the first, second and third stage of decomposition, respectively. The kinetic parameters are listed in Table 4. The *–ve* values of ΔS indicate that the reactions are slow in nature, hence assisted by the wide range of decomposition temperature [17].

The IR spectra of Ni(II) complexes showed broad bands at 3544 and 3564 cm^{-1} for Ni(II) complexes **2** and **3**, respectively, attributable to non-coordinated water molecule. There are strong absorption bands at 3247 and 3326 cm^{-1} for complexes **2** and **3**, respectively, which are assigned to υ_{NH} of the secondary amine. The IR spectrum of the thiocyanate Ni(II) complex **3** shows a strong band at 2091 cm^{-1} and medium intensity bands at 787 and 470 cm^{-1}, attributed to $\upsilon_{C=N}$, $\upsilon_{C=S}$ and υ_{NCS} bending vibration, respectively [18]. The position of these bands suggest the monodentate behaviour of N-bonded thiocyanate group [18]. The absence of the stretching and deformation frequencies for NH_2 and C=O groups of the *o*-phenylenediamine and formaldehyde, respectively indicates the formation of macrocyclic complex via the nitrogen atoms of NH group for complex **2**. For complex **3**, the presence of a new strong band at 1587 cm^{-1} confirm the formation of macrocyclic complex via the nitrogen atom of the azomethine group.

The room temperature magnetic moment measurements indicated that the Ni(II) complexes are paramagnetic (μ_{eff}=3.17 and 3.01 BM) for complexes **2** and **3** respectively, hence the Ni(II) would acquire octahedral geometry. The Nujol mull electronic spectra of these complexes are characterized by two bands at 430 and 580 nm for Ni(II)–complex **2** and 440 and 560 nm for Ni(II)–complex **3**. These bands are assigned to $^3A_{2g}\rightarrow{}^3T_{1g}(F)$ and $^3A_{2g}(F)\rightarrow{}^3T_{1g}(P)$ transitions of the Ni(II) in an octahedral configuration.

Conclusions

The results of elemental, thermal analysis, conductance and magnetic moment measurements as well as the spectral data reveal that the bonding of the metal ion to the ligands in the macrocyclic complexes can be represented as follows:

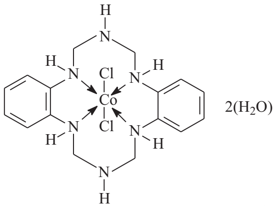
Complex (**1**)

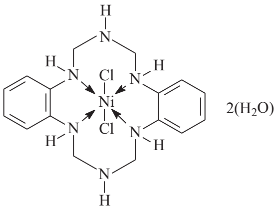
Complex (**2**)

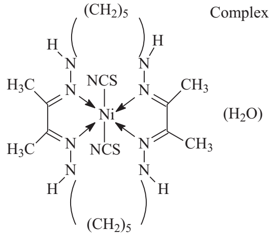
Complex (**3**)

All the complexes undergo a three-stage decomposition pattern. The values of the activation energies indicate that the metal-ligand bond is very weak. The mechanism for the solid-state thermal decomposition for the different decomposition stages is suggested. The kinetic parameters of the decomposition steps are affected by the nature of the metal ion as well as the structural formula of the ligand. The entropy of activation observed with respect to the dehydration steps has small negative values. This can be explained on the premise that the first degradation step involves two simultaneous processes; the first is volatilization of the water molecules from the solid complex with positive ΔS and the second is the formation of more ordered anhydrous complex with negative ΔS. The determined values result from both processes.

References

1 A. Chaudhary, S. Dave, S. R. Swaroop and R. V. Singh, J. Ind. Chem. Soc., 79 (2002) 371.

2 R. D. Yones, D. A. Summerville and F. Basolo, Chem. Rev., 79 (1979) 139.

3 A. Kumar Singh, R. Singh and R. Saxena, Transition Met. Chem., 29 (2004) 867 and references therein.

4 O. V. Mikhailov, M. A. Kazymova, T. A. Shumilova and S. S. Solovieva, Transition Met. Chem., 29 (2004) 732.

5 S. K. Gupta and D. Raina, Transition Met. Chem., 22 (1997) 225.

6 W. Yan, C. Ma, J. Wu, W. Zhang and D. Jang, J. Therm. Anal. Cal., 85 (1999) 393.

7 Z. Vargova, K. Györyová and V. Zelenák, J. Therm. Anal. Cal., 76 (2004) 97.

8 D. H. Busch and J. C. Bailar, J. Am. Chem. Soc., 78 (1956)1137.

9 A. W. Coats and J. P. Redfern, Nature, 20 (1964) 68.

10 V. Satava, Thermochim. Acta, 2 (1971) 423.

11 W. J. Geary, Coord. Chem. Rev., 7 (1971) 81.

12 M. K. M. Nair and P. K. Radhakrishnan, J. Thermal Anal., 52 (1998) 475.

13 C. R. Vinodkumar, M. K. M. Nair and P. K. Radhakrishnan, J. Therm. Anal. Cal., 61 (2000) 143.

14 T. Ganga Devi, K. Muraleedharan and M. P. Kannan, Thermochim. Acta, 191 (1991) 105.

15 B. N. Figgis and J. Lewis, 'Progress in Inorganic Chemistry', Interscience, New York 1964, 6, p. 37.

16 I. Fidone and K. W. Stevens, Proc. Phys. Soc., London, 73 (1959) 116.

17 M. M. Omar, J. Therm. Anal. Cal., 68 (2002) 1003.

18 K. Nakamoto, Infrared Spectra of Inorganic and Coordination Compounds, Wiley, Interscience, New York 1970.

Received: June 16, 2007
Accepted: July 11, 2007

DOI: 10.1007/s10973-007-8609-3